Journal of Reproduction and Development, Vol. 64, No 2, 2018

—Original Article—

Identification of quantitative trait loci associated with the susceptibility of mouse spermatozoa to cryopreservation

Jinsha LIU[1, 2], Keiji MOCHIDA[1], Ayumi HASEGAWA[1], Kimiko INOUE[1, 2] and Atsuo OGURA[1–3]

[1]*RIKEN BioResource Center, Ibaraki 305-0074, Japan*
[2]*Graduate School of Life and Environmental Science, University of Tsukuba, Ibaraki 305-8572, Japan*
[3]*The Center for Disease Biology and Integrative Medicine, Faculty of Medicine, University of Tokyo, Tokyo 113-0033, Japan*

Abstract. Although it is known that the susceptibility of mouse spermatozoa to freezing-thawing varies greatly with genetic background, the underlying mechanisms remain to be elucidated. In this study, to map genetic regions responsible for the susceptibility of spermatozoa to freezing-thawing, we performed *in vitro* fertilization using spermatozoa from recombinant inbred mice derived from the C57BL/6J and DBA/2J strains, whose spermatozoa showed distinct fertilization abilities after freezing. Genome-wide interval mapping identified two suggestive quantitative trait loci (QTL) associated with fertilization on chromosomes 1 and 11. The strongest QTL on chromosome 11 included 70 genes at 59.237260–61.324742 Mb and another QTL on chromosome 1 included 43 genes at 153.969506–158.217850 Mb. These regions included at least 15 genes involved with testicular expression and possibly with capacitation or sperm motility. Specifically, the *Abl2* gene on chromosome 1, which may affect subcellular actin distribution, had polymorphisms between C57BL/6J and DBA/2J that caused at least three amino acid substitutions. A correlation analysis using recombinant inbred strains revealed that the fertilization rate was strongly correlated with the capacitation rate of frozen-thawed spermatozoa after preincubation. This result is consistent with the fact that C57BL/6J frozen-thawed spermatozoa recover their fertilization capacity following treatment with methyl-β-cyclodextrin to enhance sperm capacitation. Thus, our data provide important clues to the molecular mechanisms underlying cryodamage to mouse spermatozoa.

Key words: Cryopreservation, *In vitro* fertilization, Mouse, QTL, Spermatozoa

(**J. Reprod. Dev. 64:** 117–127, 2018)

In mice, assisted reproductive technologies (ARTs) have been used extensively since the 1970s for producing offspring and preserving gametes and embryos [1–3]. Conventional ARTs in mice include superovulation, *in vitro* fertilization (IVF), embryo culture, embryo transfer, and sperm/embryo cryopreservation [4, 5]. Because of the rapid increase in the number of genetically modified mouse strains, the contribution of sperm cryopreservation as a simple and economical method for preserving genetic materials has become a major priority in many laboratories and mouse-breeding facilities [6–8]. However, spermatozoa can be damaged by freezing-thawing, specifically by cold shock [9], osmotic injury, and oxidative stress, resulting in deleterious changes to sperm motility, viability, and acrosome and membrane integrity [10].

It is noteworthy that spermatozoa from different mouse strains can show different rates of survival and motility after freezing, causing diverse efficiencies in the ARTs in terms of the production of embryos using frozen-thawed spermatozoa [11, 12]. This diverse outcome is possibly attributable to differential regulation of multiple genes, such as quantitative trait loci (QTL), which may be involved in complex mechanisms involved in sperm physiology, such as those controlling membrane integrity and motility. For example, C57BL/6 inbred mice show a low IVF rate with frozen-thawed spermatozoa [13], whereas this strain is particularly important as a standard genetic background for many transgenic and knockout strains [14]. In contrast, spermatozoa from the DBA/2 strain of mice, which has a long history as a classic inbred strain, are more resistant to freeze-thawing procedures and maintain a high capacity for fertilization [15]. This strain, specificity in its sperm's susceptibility to freezing, is evident even with R18S3, one of the most reliable sperm-freezing solutions [16]. Choi and Toyoda (1998) reported that methyl-β-cyclodextrin (MBCD) in the sperm preincubation medium could stimulate cholesterol efflux from the plasma membrane [17], and this is an important step for normal sperm capacitation [18]. The presence of L-glutamine in the R18S3 medium and MBCD in sperm preincubation medium has also been reported to greatly improve the fertilization rates using frozen-thawed spermatozoa in C57BL/6J (B6J) mice [19–21]. IVF in B6J mice was further improved by the addition of reduced glutathione (GSH) in the fertilization medium, which might promote sperm penetration through the zona pellucida [22, 23].

Thus, cryopreservation of spermatozoa from the B6 strain and its gene-modified strains can now be performed safely and might not

Received: November 10, 2017
Accepted: December 2, 2017
Published online in J-STAGE: December 21, 2017

Correspondence: A Ogura (e-mail: ogura@rtc.riken.go.jp)

need to be a research subject in a practical sense. However, there is very little information on the genes or molecular mechanisms that are responsible for strain-dependent differences in the susceptibility of spermatozoa to freezing-thawing. This kind of information would help us to better understand the unique characters of sperm physiology that are evolutionally specialized for fertilizing oocytes effectively. For this purpose, we performed QTL analysis using a set of recombinant inbred (RI) mouse strains derived from two parental inbred strains, B6J and DBA/2J (D2J), the so-called BXD RI strains [24, 25]. In general, the RI mouse strains are derived from two inbred strains through brother–sister mating of the F2 generations. Their chromosomal content forms a mosaic of genomic blocks, each alternatively inherited from one of the parents, which allows us to identify the QTLs of interest statistically. In this study, we undertook a series of IVF experiments, sperm motility tests, and sperm staining for the examination of plasma membrane integrity, acrosomal status, and capacitation using spermatozoa from BXD RI strains and their parental strains. To perform the QTL analysis efficiently, we employed an IVF procedure without using MBCD or GSH in the medium, thereby helping to delineate phenotypic differences between the strains analyzed. The IVF rates can be affected by the motility, membrane integrity, and the acrosomal and capacitation statuses of spermatozoa before fertilization. Therefore, we also examined these sperm-related parameters in RI strains to determine whether there were correlations between the fertilization rate and these sperm-related parameters.

Materials and Methods

Mice

Male mice (> 12 weeks of age) of eight BXD RI strains and the D2J strain were provided by the RIKEN BioResource Center. Male and female B6J mice were purchased from Charles River Japan (males > 12 weeks, females > 9 weeks). At least six male mice of each strain were used for each IVF experiment and motility test (i.e., six replicates). We used another set of male mice for sperm staining. Female B6J mice were used to collect mature oocytes. All mice were housed with food and water provided *ad libitum* under controlled temperature (24 ± 1°C), humidity (55 ± 2%) and lighting conditions (daily light period, 0700 to 2100 h). All experiments were approved by the Animal Experimentation Committee at the RIKEN Tsukuba Institute and were performed in accordance with the committee's guiding principles.

IVF

IVF was performed as previously described with slight modifications [26]. For IVF using fresh spermatozoa, the male mice were killed by cervical dislocation and both epididymides were promptly collected. Blood was removed from the epididymal surface with filter paper and a sperm mass was collected by puncturing the cauda. This was suspended in a drop of 450 µL human tubal fluid (HTF) [27] containing 0.3% bovine serum albumin (BSA), covered with mineral oil, and preincubated at 37°C under 5% CO_2 in humidified air for 1 h. Female B6J mice were induced to superovulate with an intraperitoneal injection of 7.5 IU of equine chorionic gonadotropin (eCG; Peamex, Sankyo, Tokyo, Japan), followed 48–50 h later by 7.5 IU of human chorionic gonadotropin (hCG; Gonatropin; ASKA Pharmaceutical, Tokyo, Japan). Cumulus–oocyte complexes were placed into 80 µl drops of HTF medium covered with sterile mineral oil. Insemination was carried out by adding preincubated spermatozoa to the fertilization medium containing oocytes. IVF experiments were also performed using frozen-thawed spermatozoa, as described below. The final sperm concentrations were adjusted to 2.0×10^5 and 5.0×10^5 cells/ml for fresh and frozen-thawed spermatozoa, respectively. At 5 h after insemination, the oocytes were removed from the fertilization medium and washed in CZB medium containing glucose [28]. They were fixed with 2.5% glutaraldehyde and stained with 1% aceto-orcein to visualize pronuclei [29]. The oocytes with a male pronucleus or pronuclei and sperm tail(s) in the cytoplasm were considered to be fertilized irrespective of the number of penetrating spermatozoa.

Freezing and thawing of spermatozoa

Spermatozoa were frozen-thawed according to the method developed by Nakagata and Takeshima (1993) with slight modifications. The sperm cryopreservation solution (R18S3) consisted of 18% raffinose (Difco, Becton Dickinson, Franklin Lakes, NJ, USA) and 3% skim milk (Difco, Becton Dickinson). Fat and blood were removed from each epididymis on filter papers using fine scissors. Approximately 10 epididymal incisions were made with sharp scissors under 100 µl R18S3, and the resulting sperm suspension was divided into eight 10 µl aliquots. Each of these was aspirated into a 0.25 ml plastic straw and cooled in liquid nitrogen (LN_2) vapor for 10–60 min before submersion in LN_2. The spermatozoa were stored in LN_2 for at least 1 week before thawing. For thawing, the straws were removed from the LN_2, exposed to ambient temperature for 10 sec and then immersed in a water bath at 37°C for 15 min. An aliquot of 5 µl thawed sperm suspension was taken from the periphery of the drop and added to 200 µl of HTF medium for preincubation and used for IVF as described above.

Assessment of sperm motility

For sperm motility analysis, we used computer-aided spermatozoa analysis (CASA) with a Hamilton Thorn IVOS CASA analyzer (Hamilton Thorn Research, Beverley, MA, USA) to record quantitative parameters of sperm motion. Spermatozoa were incubated in droplets of 450 µl (fresh spermatozoa) or 200 µl (frozen spermatozoa) of HTF medium containing 0.3% BSA for 1 h at 37°C. Before collection of spermatozoa, the incubation drops were stirred so that the average sperm population could be used for analysis. The sperm motility rate was recorded by counting cells with any movement of the head and the progressive motility rate was recorded by counting those with a velocity > 50 µm/sec. In addition, at least 300 spermatozoa per sample were analyzed for curvilinear velocity (VCL, µm/sec), average path velocity (VAP, µm/sec), straight-line velocity (VSL, µm/sec), linearity (LIN), amplitude of lateral head displacement (ALH, µm), and straightness (STR).

Assessment of plasma membrane integrity and the acrosome status of frozen-thawed spermatozoa

Plasma membrane integrity and the acrosomal status of frozen-thawed spermatozoa were assessed by propidium iodide (PI) and

peanut agglutinin (PNA) staining, respectively, as previously described [30]. Briefly, after preincubation of thawed spermatozoa for 1 h, a 20 µl aliquot of suspension was placed in a tube and stained with 1 µl of lectin peanut agglutinin (PNA) conjugated with Alexa Fluor 488 (1 mg/ml, Invitrogen, Paisley, UK) mixed with 0.5 µl of PI (2.4 mM, LIVE/DEAD® Sperm Viability Kit; Molecular Probes, Eugene, OR, USA) without fixation. The tube was incubated in a dark box at 37°C for 15 min. After incubation, 100 spermatozoa per sample were observed under a fluorescent microscope and classified into three staining patterns: PI(+), PI(–)/PNA(–), and PI(–)/PNA(+). PI(+) represents dead spermatozoa and PI(–)/PNA(–) represents live spermatozoa with an intact acrosome. PI(–)/PNA(+) represents live spermatozoa ready to undergo the acrosome reaction; this state allows PNA to reach the acrosomal contents through pores in the outer acrosomal membrane and plasmalemma.

Assessment of capacitation status

After preincubation of the thawed sperm suspension for 1 h, an aliquot of 20 µl was put in a tube and stained with an equal volume of chlortetracycline (CTC) solution prepared by dissolving 750 mM CTC-HCl (Sigma-Aldrich, St Louis, MO, USA) in a chilled buffer containing 20 mM Tris–HCl, 130 mM NaCl, and 5 mM cysteine-HCl (pH 7.0) [31–33]. After mixing, spermatozoa were fixed by adding 5 µl of 1% glutaraldehyde in 1 M Tris HCl (pH 8.0) [17]. Totals of at least 600 spermatozoa per strain were observed under a fluorescence microscope and classified into three patterns according to Ward and Storey (1984): the F pattern indicated uniform fluorescence over the head (uncapacitated); B pattern showed fluorescence on the anterior portion of the head and a dark band over the postacrosomal region (capacitated but not acrosome-reacted); and AR pattern showed no or little fluorescence over the entire surface of the head (capacitated and acrosome-reacted). The B pattern was considered representative of a normal sperm population at the end of preincubation.

QTL analysis

All QTL mapping for phenotypes was performed using the WebQTL software module of the GeneNetwork (www.genenetwork.org) [34]. Interval mapping to evaluate potential QTLs was calculated from the likelihood ratio statistics (LRS) as the software's default measurement of the association between differences in traits and differences in particular genotype markers. Another common measure score, the log of the odds (LOD) ratio, can be converted from the LRS (LRS/4.61). Suggestive and significant LRS values were determined by applying 1000 permutations. Assessments of QTL peaks and shoulders that cross the suggested threshold were performed using QTL miner, which was implemented in the GeneNetwork package (http://genenetwork.helmholtz-hzi.de) to identify regulating genes [35, 36]. We scrutinized the genes mapped within the analyzed QTLs by the National Center for Biotechnology Information (NCBI) Entrez Gene website (http://www.ncbi.nlm.nih.gov/sites/entrez?db=gene) and the Jackson Laboratory's Mouse Genome Database (MGI) project (www.informatics.jax.org) to identify potential candidate genes.

Statistical analysis

All results are expressed as the mean ± standard error of the mean (SEM). Percentile data were transformed by the arcsine transformation and analyzed by two-way analysis of variance (ANOVA) using Excel software. The Tukey-Kramer test was used for multiple comparisons of the fertilization rate and sperm-related parameters, except for those with non-normal distributions. For those parameters with non-normal distributions (motile rate, ALH, LIN, and PI(–)/PNA(+) rate), the Kruskal-Wallis test was applied for multiple comparisons. Correlations between mean parameter values in B6J, D2J, and BXD RI mice were analyzed using Pearson's correlation coefficient by applying R, a free software environment for statistical computing and graphics (http://www.R-project.org).

Results

Fertilizing abilities of fresh and frozen-thawed spermatozoa from the B6J, D2J, and BXD RI mouse strains

We used B6J strain oocytes in our IVF experiments throughout to exclude the effects of oocyte-related factors on the fertilization rates using different sources of spermatozoa. Oocytes with a male pronucleus (or pronuclei) and with sperm tails in the cytoplasm at 5 h after insemination were considered to be fertilized (penetrated) irrespective of the number of penetrating spermatozoa (Fig. 1A). First, we examined whether the B6J strain spermatozoa were more susceptible to freeze-thawing than the D2J spermatozoa, as has been previously reported [12]. A two-way ANOVA with a 2 × 2 factorial design for B6J *vs*. D2J strains and fresh *vs*. frozen-thawed sperm suspensions revealed that both factors had significant effects on the fertilization rate (Table 1). There was an interaction between the two factors (strain and freeze-thawing), indicating that the fertilization rate was determined by a combination of these factors as well. A multiple comparison test revealed that that B6J spermatozoa were more sensitive to freeze-thawing than D2J spermatozoa (Fig. 1B and Table 1). This result corroborates a report of strain-specific variation in the susceptibility to cryopreservation [12]. Then, we undertook large-scale IVF experiments using fresh and frozen-thawed spermatozoa from all the RI strains under strictly controlled conditions. The fertilization rates in all the experiments are shown in Table 2. As expected, the fertilization rates of seven out of eight RI strains were within the range of values for the B6J and D2J strains (Fig. 1C).

QTL mapping for genetic regions associated with cryodamage to spermatozoa

Genome-wide interval mapping with the fertilization rates using frozen-thawed spermatozoa detected only one suggested QTL on chromosome 1 above the threshold LRS score (8.52) (Fig. 2A). Although there was another peak on chromosome 11, it was under the threshold LRS score. There were also many other near-threshold peaks over the entire genome. From the results from the two-way ANOVA described above, we assumed that the fertilization rates using frozen-thawed spermatozoa might be determined by strain-specific susceptibility to freezing, as well as the intrinsic fertilizing ability of the strain. Therefore, the results of the QTL analysis based on the fertilization rates of frozen-thawed spermatozoa might have reflected the cumulative effect of these two factors. To exclude the possible background strain effects, we calculated the ratio of the fertilization rate of frozen-thawed spermatozoa per that of fresh spermatozoa in individual male mice (designated here as "relative

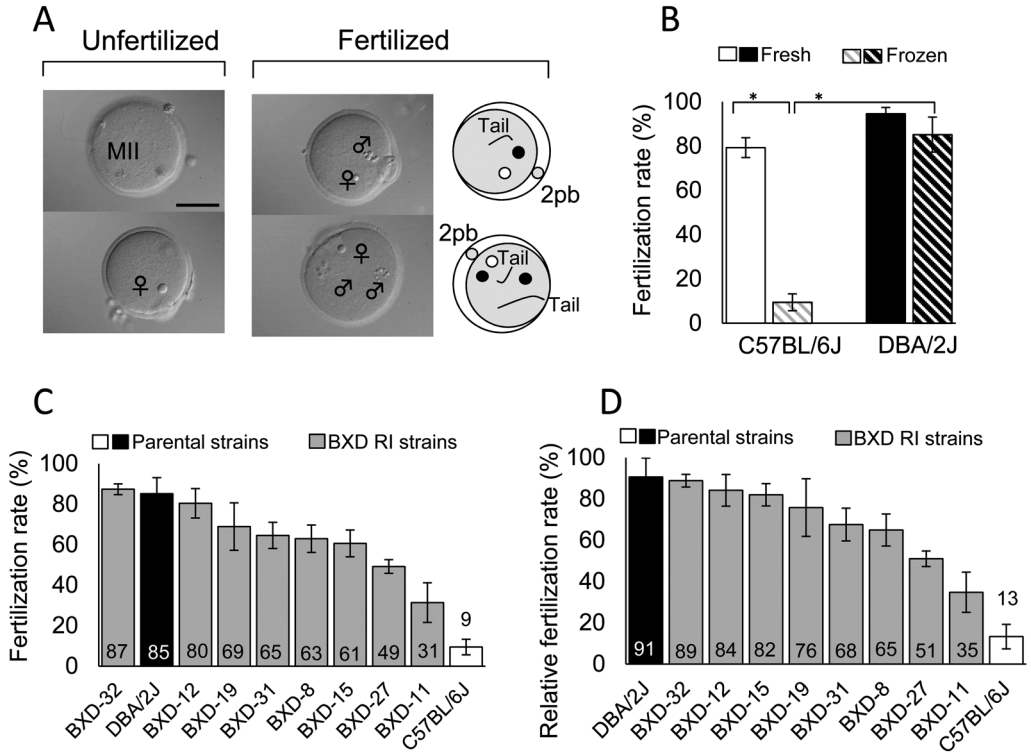

Fig. 1. Fertilization rates of fresh and frozen-thawed spermatozoa from RI, B6J, and D2J mouse strains. (A) Oocytes at 5 h post-insemination subjected to aceto-orcein staining. Fertilized oocytes can contain one or more spermatozoa within the ooplasm. 2pb, the second polar body; bar = 50 μm. (B) Fertilization rates using fresh or frozen-thawed spermatozoa from B6J and D2J mouse strains (means ± SEMs; * $P < 0.01$ by Tukey-Kramer test). See Table 1 for the result of two-way ANOVA. (C) Strain distribution of the fertilization rates using frozen-thawed spermatozoa from the RI, B6J, and D2J mouse strains (means ± SEMs). (D) Strain distribution of the relative fertilization rates using frozen-thawed spermatozoa from RI, B6J, and D2J strains of mice (means ± SEMs). The values were calculated by the fertilization rate of frozen-thawed spermatozoa divided with that of fresh spermatozoa in each individual male; Relative fertilization rate (%) = (Fertilization rate with frozen spermatozoa (%)/Fertilization rate with fresh spermatozoa (%)) × 100 (n = 6 for each strain).

fertilization rate"). As shown in Fig. 1D, the relative fertilization rates of all eight RI strains were within the range of values for B6J and D2J. QTL analysis based on the relative fertilization rates made the genome-wide interval mapping more explicit: two suggested QTLs on chromosomes 1 and 11 were detected and most of the near-threshold peaks disappeared from the map (Fig. 2B).

Candidate genes that might determine the relative fertilization rate

To identify candidate genes that might determine the strain-specific relative fertilization rate, we used the QTL miner tool in GeneNetwork. The corresponding genetic region of 153.969506–158.217850 Mb on chromosome 1 contained 43 genes, and the region of 59.237260–61.324742 Mb on chromosomes 11 contained 70 genes [35] (Supplementary Table 1: online only). We selected candidate genes on these regions based on the following two criteria: (1) genes expressed in the testis, using NCBI mouse ENCODE transcriptome data; and (2) genes expressed in the reproductive system in the phenotype annotation of MGI Mouse Genome Database from the Jackson Laboratory. Furthermore, we added candidate genes with the following keywords in the MGI database based on essential roles of intrinsic Ca^{2+}-ATPase activity during capacitation [32]. This reflects the energy production in mitochondria for spermatozoa during the transition from progressive to hyperactivated motility [37] and cholesterol depletion from the plasma membrane during capacitation [18]. These genes are involved in: (1) calcium channel activity in the Gene Ontology (GO) terms from MGI; (2) ATP binding sites based on protein information in MGI; and (3) cholesterol metabolic process in GO. Finally, 15 candidate genes were selected with these criteria, as listed in Table 3. Of them, seven genes have sequence polymorphisms on exons between B6J and D2J and two have amino acid substitutions (Table 3).

Motility of fresh and frozen-thawed spermatozoa from B6J, D2J, and BXD RI strains

We obtained nine sperm motility parameters by CASA (Table 4). The 2 × 2 factorial ANOVA using B6J *vs*. D2J and fresh *vs*. frozen spermatozoa indicated that both factors (strain and freeze-thawing) had significant effects on the progressively motile rate, VAP, VSL, and VCL (Table 1). There was an interaction between two factors in VSL, indicating that this parameter was determined by the combination of the strain and freeze-thawing treatment (Table 1). We did not apply

Table 1. Probability (P-values) of main effects on phenotypes analyzed by two-way ANOVA in C57BL/6J (B6J) and DBA/2J (D2J) mice

	Main effect		Interaction (Strain × Freezing)	Multiple comparison test
	Strain (B6J, D2J)	Freezing (Fresh, Frozen)		
Fertilization [a)]	**<0.0001**	**<0.0001**	**0.0006**	Tukey-Kramer
Monospermic [a)]	**<0.0001**	**<0.0001**	**<0.0001**	Tukey-Kramer
Motile [b)]	NA	NA	NA	Kruskal-Wallis
Progressively motile [b)]	**0.0120** (D2J > B6J)	**<0.0001** (Fresh > Frozen)	0.1607	
VAP [b)]	**<0.0001** (D2J > B6J)	**<0.0001** (Fresh > Frozen)	0.1577	
VSL [b)]	**<0.0001**	**0.0002**	**0.0307**	Tukey-Kramer
VCL [b)]	**<0.0001** (D2J > B6J)	**<0.0001** (Fresh > Frozen)	0.2448	
ALH [b)]	NA	NA	NA	Kruskal-Wallis
BCF [b)]	**0.0072** (D2J < B6J)	0.5105	0.0916	
LIN [b)]	NA	NA	NA	Kruskal-Wallis
STR [b)]	0.1165	0.7366	**0.0258**	
PI (–) [c)]	**0.0097** (D2J > B6J)	**<0.0001** (Fresh > Frozen)	0.0979	
PI(–)/PNA(+) [c)]	NA	NA	NA	Kruskal-Wallis
F pattern [d)]	**0.0337**	**0.0067**	**0.0044**	Tukey-Kramer
B pattern [d)]	**0.0493**	**0.0023**	**0.0175**	Tukey-Kramer
AR pattern [d)]	0.7615	0.2299	0.5822	
Capacitation [d)]	**0.0337**	**0.0067**	**0.0044**	Tukey-Kramer

A probability of $P < 0.05$ was considered significant (boldface). [a)] Fertilized oocytes may contain one or more spermatozoa within the ooplasm. The monospermic fertilization rate was the rate of oocytes containing only one male pronucleus per oocyte examined. [b)] Motility parameters are as follows: The percentage of motile and progressive motile spermatozoa; VAP, average path velocity; VSL, straight-line velocity; VCL, curvilinear velocity; ALH, amplitude of lateral head displacement; BCF, beat-cross frequency; STR, straightness; LIN, linearity. [c)] Spermatozoa stained with PI and PNA. PI(–) indicates spermatozoa with intact plasma membrane. PI(–)/PNA(+) indicates live spermatozoa ready for acrosome reaction. [d)] Spermatozoa stained with CTC. F pattern shows uniform fluorescence over the head (uncapacitated). B pattern shows fluorescence on the anterior portion of the head and a dark band over the postacrosomal region (capacitated but non-acrosome-reacted). AR pattern shows no or little fluorescence over the whole surface of the head (capacitated and acrosome-reacted). Both B pattern and AR pattern spermatozoa are considered to be capacitated. NA, not available because of a non-normal distribution (the results of multiple comparison test by Kruskal-Wallis test are shown in Tables 4 or 5).

factorial analysis to the motile rate and ALH or LIN values, because they did not follow a normal distribution. The multiple comparison test revealed that the freezing-thawing procedure significantly decreased the progressively motile rate, VAP, VSL, and VCL (Fig. 3 and Table 1). Therefore, we subjected these four sperm motility parameters to an analysis of correlation with the relative fertilization rate.

Plasma membrane integrity and acrosomal status of spermatozoa from B6J, D2J, and BXD RI strains

Next, we examined the structural integrity of the plasma membrane and acrosome by staining with PI and PNA, which are localized in the nucleus and the acrosome [30], respectively. PI staining classified spermatozoa into membrane-damaged (PI(+)) or membrane-intact (PI(–)) (Fig. 4A). The PI(–)/PNA(+) pattern indicated live spermatozoa ready to undergo the acrosome reaction (Fig. 4A). The 2 × 2 factorial ANOVA using B6J and D2J strains showed that both strain and freeze-thawing treatment had significant effects on the integrity of the plasma membrane of spermatozoa, but there was no interaction between them (Fig. 4B, PI(–) in Table 1). However, PI(–)/PNA(+) was not applied for factorial analysis because it did not follow a normal distribution (Table 1). The multiple comparison test for these parameters revealed that the freezing-thawing procedure showed significant differences in the PI(–) and PI(–)/PNA(+) in B6J spermatozoa, indicating that the proportions of spermatozoa with intact plasma membrane and acrosome decreased in B6J mice (Table 1 and Fig. 4C). Data from spermatozoa of the RI and parental strains are shown in Table 5.

Capacitation status of spermatozoa from B6J, D2J, and BXD RI strains

The capacitation status was determined by the fluorescent pattern of CTC that detects intracellular Ca^{2+}-related changes in the spermatozoa [32]. The F and B patterns that indicated the uncapacitated status and capacitated, but nonacrosome-reacted status, respectively, were affected by both strain and freezing-thawing (Fig. 4D and Table 1). However, the AR pattern that indicates capacitated and acrosome-reacted status was not affected by these factors (Fig. 4D and Table 1). The rate of capacitated spermatozoa comprising the B and AR patterns was affected by the two factors (Fig. 4D and Table 1). There were interactions between these factors in the F and B patterns and capacitation (Table 1). The multiple comparison test in these parameters revealed that the freezing-thawing procedure resulted in a significant reduction in the capacitation rate in the B6J strain, indicating that B6J spermatozoa were more sensitive to

Table 2. Fertilization rates of fresh and frozen-thawed spermatozoa from C57BL/6J, DBA/2J, and BXD RI mice

Strain	No. of males	Spermatozoa	No. of oocytes	Fertilization (%)	Monospermic fertilization (%)
C57BL/6J	6	Fresh	183	79.3 ± 4.5 [a]	73.8 ± 2.7 [a]
	6	Frozen	205	9.4 ± 3.8 [bc]	9.4 ± 3.8 [bc]
	6	Relative		13.3 ± 6.0	
DBA/2J	6	Fresh	212	94.6 ± 2.8	80.6 ± 4.1
	6	Frozen	207	85.2 ± 7.9 [d]	70.3 ± 7.9 [d]
	6	Relative		90.6 ± 9.2	
BXD-8	6	Fresh	186	97.5 ± 1.3	85.3 ± 3.9
	6	Frozen	198	63.0 ± 6.8	62.0 ± 6.5
	6	Relative		64.9 ± 7.8	
BXD-11	6	Fresh	176	89.4 ± 5.0	84.2 ± 6.0
	6	Frozen	204	31.4 ± 9.8	31.0 ± 9.8
	6	Relative		34.8 ± 9.8	
BXD-12	6	Fresh	206	95.7 ± 1.4	85.9 ± 1.3
	6	Frozen	188	80.5 ± 7.3	80.5 ± 7.3
	6	Relative		84.2 ± 7.66	
BXD-15	6	Fresh	221	73.3 ± 6.4	71.0 ± 5.8
	6	Frozen	212	60.6 ± 6.6	59.7 ± 6.5
	6	Relative		82.0 ± 5.4	
BXD-19	6	Fresh	198	93.1 ± 3.5	90.2 ± 2.5
	6	Frozen	184	68.9 ± 12.0	67.9 ± 11.3
	6	Relative		75.8 ± 14.0	
BXD-27	6	Fresh	212	96.8 ± 1.5	87.5 ± 3.2
	6	Frozen	186	49.2 ± 3.4	49.2 ± 3.4
	6	Relative		51.0 ± 3.8	
BXD-31	6	Fresh	203	96.4 ± 2.0	93.2 ± 2.3
	6	Frozen	187	64.6 ± 6.5	64.1 ± 6.3
	6	Relative		67.6 ± 7.9	
BXD-32	6	Fresh	192	98.5 ± 0.70	82.1 ± 4.1
	6	Frozen	206	87.4 ± 2.70	76.1 ± 3.0
	6	Relative		88.8 ± 3.08	

Values are means ± SEMs. Different superscripts within the same column indicate significant differences ([a, b; c, d] $P < 0.01$, two-way ANOVA followed by Tukey-Kramer test, see Table 1). Relative fertilization rate (%) = (Fertilization rate with frozen spermatozoa (%)/Fertilization rate with fresh spermatozoa (%)) × 100 (n = 6 for each strain).

freezing-thawing than the D2J spermatozoa in terms of their ability to undergo capacitation (Fig. 4E). Data from spermatozoa of the RI and parental strains are shown in Table 5.

Correlations of the fertilization rate with other parameters

To understand the relationship among parameters we examined, we tested for correlations among phenotypes of frozen-thawed spermatozoa in BXD RI and parental strains. We used the major motility, membrane integrity, and capacitation parameters that were significantly different between B6J and D2J mice. For exact correlation analysis, these sperm-related parameters were also transformed into relative values by dividing with the corresponding values from fresh spermatozoa. Overall, the relative fertilization rate was most highly correlated with the B pattern of CTC staining (capacitated but not acrosome-reacted), followed by PI(–)/PNA(+) staining (live spermatozoa ready to undergo acrosome reaction) (Fig. 5). Their correlations were statistically significant (Pearson's correlation, $r > 0.64$, $P = 0.027$ and 0.039, respectively). Other parameters had no significant correlation with the relative fertilization rates. The sperm motility parameters had especially low correlation values, although they were highly correlated with each other (Fig. 5).

Discussion

The primary purpose of our study was to identify loci responsible for strain differences in the susceptibility of mouse spermatozoa to freezing-thawing. As the B6J and D2J strains are known to exhibit distinct phenotypes in terms of the fertilization rates using frozen-thawed spermatozoa [12], the RI strains derived from these two parental strains would provide the best model for the QTL analysis for such responsible loci. In this study, however, only eight RI strains could be used because of the limited number of strains available at our center. This was much smaller than those of other studies using the similar BXD RI strains [36, 38]. Despite the small number of strains, we successfully identified two responsible QTLs on chromosomes 1 and 11. This was probably because of the large strain-specific difference between parental strains in the susceptibility of spermatozoa to freezing-thawing; it is generally known that a broad range of values among strains increases the efficiency of QTL analysis based on RI strains [39]. We found that the use of "relative fertilization rate" as a parameter could also be attributed to responsible QTLs, as shown by the more distinct profile of the genome-wide mapping of the relative fertilization rate compared with that of the fertilization rate with frozen-thawed spermatozoa (Fig. 2A, B).

The suggestive QTLs on chromosomes 1 and 11 allowed us to identify 15 candidate genes that could cause strain-specific differences in the fertilizing ability of frozen-thawed spermatozoa. We confirmed that at least four and three of the genes on chromosome 1 and chromosome 11, respectively, possessed a single nucleotide polymorphism between B6J and D2J strains, according to the MGI database. Of them, *Abl2* on chromosome 1 and *Nlrp3* on chromosome 11 have amino acid substitutions (Table 3). The Abl2 protein (or Arg) is known to coordinate actin remodeling as a key regulator of subcellular structures [40]. Therefore, there is a possibility that this gene could cause the cryotolerance specific for spermatozoa from the D2J strain. The Nlrp3 protein is a member of the family of Nod-like receptor (NLR) proteins, which are involved in the immune system, helping to start and regulate the immune system's response to injury, toxins, or invasion by microorganisms [41]. A gene knockout study revealed that Nlrp3 was involved in spermatogenic defects as a consequence of testicular ischemia and reperfusion [42]. However, we do not know whether Nlrp3 may affect the degree of cryoinjury of spermatozoa. Future studies using congenic strains or gene-edited mice carrying point mutations of these genes would provide a clear answer to this question.

Our analysis using CTC staining revealed that B6J spermatozoa showed a remarkably decreased ability to undergo capacitation after freezing-thawing, showing a sharp contrast with D2J spermatozoa, which were not affected by the same treatment. This was consistent with the finding that the efficiency of IVF using frozen-thawed B6J spermatozoa was efficiently improved by preincubation of sperm

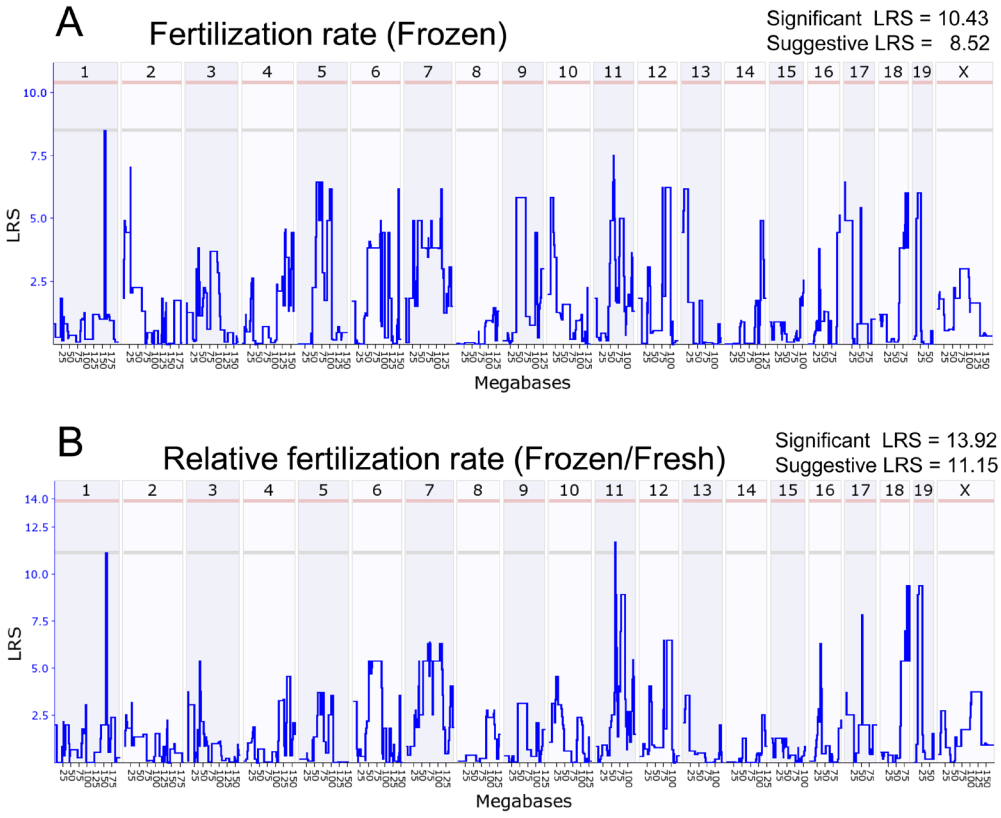

Fig. 2. Genome-wide interval mapping for suggestive QTLs affecting the fertilization rate using frozen-thawed spermatozoa. (A) Mapping based on the actual fertilization rates. (B) Mapping based on the relative fertilization rates. Critical intervals were selected based on peak shapes and bootstrap signals. Interval mapping is shown across the entire genome as a blue line representing the LRS scores. The x-axis shows physical maps in megabases for each chromosome. The y-axis represents the LRS score. The numbers along the top of the graph indicate individual chromosome numbers. The horizontal lines mark the genome-wide significant thresholds at $P < 0.05$ (red line) and suggestive thresholds at $P < 0.37$ (gray line).

Table 3. List of genes within suggestive QTLs for the relative fertilization rate

Symbol	Chr	Keywords	Testis/RPKM	SNP on Exon	A. A. Substitution B6J/D2J (Position)
Tdrd5	1	male infertility, spermatogenesis, spermatid development	8.70	Y	–
Soat1	1	cholesterol metabolic process	7.27	Y	–
Abl2	1	reduced fertility, reproductive process, ATP binding	1.80	Y	V/A (28) A/P (32) M/V (1030)
Cacna1e	1	calcium channel	0.08	Y	–
Pld6	11	male infertility, reproductive system	33.96	–	–
Slc47a2	11	ductus deferens, epididymis	31.60	–	–
Map2k3	11	male reproductive system	13.64	Y	–
Flii	11	ductus deferens, epididymis, penis	7.28	–	–
Alkbh5	11	reduced male fertility	6.85	–	–
Usp22	11	epididymis	6.08	–	–
Rasd1	11	ductus deferens, epididymis	3.52	–	–
Wnt3a	11	reduced female fertility, ejaculatory epididymis, seminal vesicle	1.93	Y	–
Wnt9a	11	ejaculatory duct	0.23	–	–
Kcnj12	11	epididymis	0.04	–	–
Nlrp3	11	reduced fertility	0.04	Y	L/V (717)

RPKM, reads per kilobase of exon per million mapped sequence reads (http://www.ncbi.nlm.nih.gov/sites/entrez?db=gene). The gene information was obtained from Gene Expression Database in Mouse Genomics Informatics (www.informatics.jax.org). Y: Possessed a single nucleotide polymorphism between B6J and D2J strains, according to the MGI database. –: Not possess. A. A. Substitution: amino acid substitution.

Table 4. Motility of fresh and frozen-thawed spermatozoa from C57BL/6J, DBA/2J, and BXD RI mice

Strains	No. of males	Spermatozoa	Motile (%)	Progressively motile (%)	VAP (μm/sec)	VSL (μm/sec)	VCL (μm/sec)
C57BL/6J	6	Fresh	72.8 ± 3.4 [a]	40.7 ± 1.5	167.0 ± 3.4	94.5 ± 2.7 [ac]	361.2 ± 5.5
	6	Frozen	25.8 ± 1.9 [b]	12.2 ± 1.1	143.1 ± 4.1	82.2 ± 2.5 [bc]	317.9 ± 4.7
DBA/2J	6	Fresh	74.5 ± 2.0 [a]	48.7 ± 1.3	254.8 ± 2.8	164.1 ± 2.3 [ad]	551.5 ± 5.7
	6	Frozen	26.5 ± 2.5 [b]	14.0 ± 1.7	213.7 ± 2.6	126.3 ± 4.5 [db]	482.8 ± 5.5
BXD-8	6	Fresh	74.3 ± 2.9	42.8 ± 3.1	204.2 ± 7.3	126.0 ± 7.4	423.5 ± 13.7
	6	Frozen	29.8 ± 1.4	14.3 ± 0.9	172.4 ± 5.0	97.1 ± 4.0	368.9 ± 13.9
BXD-11	6	Fresh	66.7 ± 3.7	40.8 ± 2.3	211.6 ± 4.0	137.9 ± 2.9	460.8 ± 7.6
	6	Frozen	22.0 ± 2.0	11.8 ± 0.7	184.1 ± 5.0	105.9 ± 4.0	401.3 ± 6.1
BXD-12	6	Fresh	66.8 ± 3.7	39.3 ± 3.3	199.8 ± 8.4	127.1 ± 5.7	432.9 ± 15.1
	6	Frozen	24.0 ± 1.3	14.0 ± 1.0	205.3 ± 6.0	126.8 ± 5.3	439.7 ± 12.8
BXD-15	6	Fresh	71.0 ± 2.7	45.2 ± 2.5	205.9 ± 4.2	131.7 ± 4.2	416.5 ± 6.8
	6	Frozen	22.7 ± 2.9	11.2 ± 1.9	155.3 ± 9.3	86.1 ± 6.6	329.2 ± 14.7
BXD-19	6	Fresh	64.0 ± 4.5	37.7 ± 3.8	192.4 ± 7.2	121.7 ± 4.9	396.7 ± 12.3
	6	Frozen	19.5 ± 4.3	11.0 ± 2.6	167.5 ± 3.9	93.9 ± 4.7	361.1 ± 14.2
BXD-27	6	Fresh	65.0 ± 3.2	40.3 ± 2.8	229.2 ± 4.3	148.6 ± 2.9	473.4 ± 9.6
	6	Frozen	27.7 ± 2.0	15.0 ± 0.6	202.1 ± 2.9	119.8 ± 3.8	428.4 ± 6.0
BXD-31	6	Fresh	70.7 ± 1.9	45.5 ± 2.1	191.0 ± 8.1	122.9 ± 5.3	395.1 ± 17.8
	6	Frozen	20.2 ± 1.4	11.2 ± 1.0	155.3 ± 3.9	94.5 ± 4.0	331.8 ± 8.2
BXD-32	6	Fresh	75.8 ± 2.4	49.3 ± 3.2	226.7 ± 14.9	157.9 ± 12.1	465.3 ± 27.2
	6	Frozen	28.7 ± 2.0	14.8 ± 0.8	204.2 ± 4.3	119.1 ± 3.3	438.0 ± 7.8

Strains	No. of males	Spermatozoa	ALH (μm)	BCF (Hz)	LIN (%)	STR (%)
C57BL/6J	6	Fresh	21.8 ± 0.3 [a]	37.5 ± 0.6	26.7 ± 1.0	56.7 ± 1.3
	6	Frozen	22.2 ± 0.6 [a]	38.9 ± 0.7	27.5 ± 0.5	58.8 ± 1.5
DBA/2J	6	Fresh	30.1 ± 0.3 [b]	36.8 ± 2.3	29.2 ± 0.2	61.8 ± 0.3
	6	Frozen	30.0 ± 0.7 [b]	36.2 ± 0.5	26.7 ± 0.7	53.5 ± 6.5
BXD-8	6	Fresh	26.0 ± 0.5	34.1 ± 1.9	28.3 ± 0.9	58.5 ± 1.4
	6	Frozen	26.6 ± 0.6	37.7 ± 0.6	27.2 ± 0.7	56.3 ± 1.8
BXD-11	6	Fresh	27.5 ± 0.3	37.4 ± 0.5	29.2 ± 0.5	62.2 ± 0.9
	6	Frozen	26.4 ± 1.3	37.2 ± 0.5	27.2 ± 0.5	57.3 ± 1.1
BXD-12	6	Fresh	27.0 ± 0.4	35.7 ± 0.6	30.0 ± 0.3	62.7 ± 0.7
	6	Frozen	25.4 ± 0.6	35.7 ± 0.4	29.7 ± 0.5	61.0 ± 1.1
BXD-15	6	Fresh	25.0 ± 0.2	34.8 ± 0.6	31.7 ± 0.8	61.5 ± 1.0
	6	Frozen	22.4 ± 0.9	37.5 ± 0.7	27.2 ± 1.0	57.7 ± 0.9
BXD-19	6	Fresh	25.6 ± 0.4	36.5 ± 0.6	30.2 ± 0.5	61.5 ± 0.8
	6	Frozen	21.8 ± 1.7	38.6 ± 0.7	27.8 ± 0.9	58.3 ± 1.5
BXD-27	6	Fresh	28.3 ± 0.4	35.6 ± 0.6	30.8 ± 0.3	61.7 ± 0.2
	6	Frozen	27.7 ± 0.8	34.2 ± 1.1	29.0 ± 0.7	59.3 ± 0.7
BXD-31	6	Fresh	23.4 ± 0.8	36.4 ± 0.5	31.2 ± 0.4	63.0 ± 0.4
	6	Frozen	22.2 ± 1.2	37.9 ± 0.9	30.2 ± 0.4	61.2 ± 1.2
BXD-32	6	Fresh	25.6 ± 0.6	38.2 ± 0.4	31.5 ± 0.9	64.7 ± 1.2
	6	Frozen	26.8 ± 0.6	36.2 ± 0.5	28.0 ± 0.6	58.3 ± 0.7

Values are means ± SEMs. Different superscripts within the column indicate significant differences ([a, b; c, d] $P < 0.01$, for the motile rate and VSL, Kruskal-Wallis test and two-way ANOVA followed by Tukey-Kramer test were applied, respectively. See Table 1). Multiple comparisons were not applied for the progressively motile rate, VAP, and VCL because of the absence of a significant interaction between factors (see Table 1).

with MBCD, which enhances capacitation by promoting the removal of cholesterol from the sperm membrane [19].

The capacitated spermatozoa detected by CTC staining consisted of B and AR patterns. It is known that spermatozoa with the B pattern are not acrosome-reacted and those with an AR pattern are acrosome-reacted, whereas both types are capacitated. Correlation analysis revealed that the relative fertilization rate had a greater correlation with the B pattern than that of the AR pattern or capacitation (B +

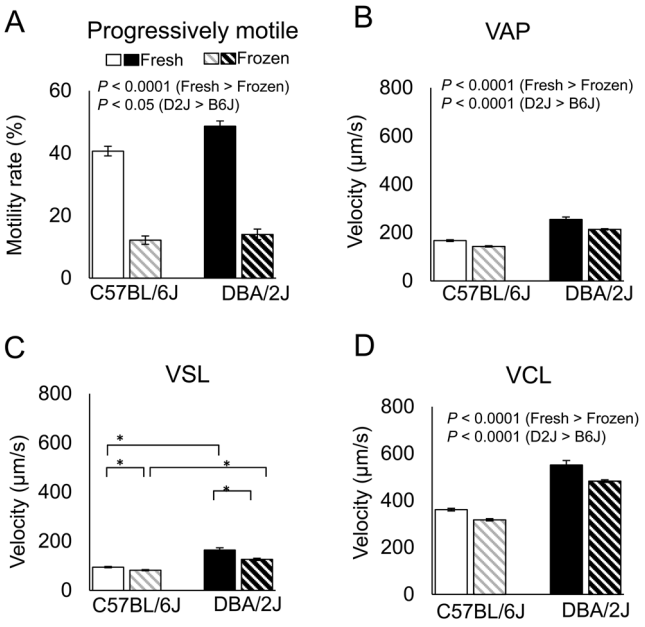

Fig. 3. Motility parameters of fresh and frozen-thawed spermatozoa from RI, B6J, and D2J strains of mice. Analysis using the parental strains (means ± SEMs; * $P < 0.01$ by Tukey-Kramer test). See Table 1 for the results of two-way ANOVA. VSL, straight-line velocity; VCL, curvilinear velocity; VAP, average path velocity.

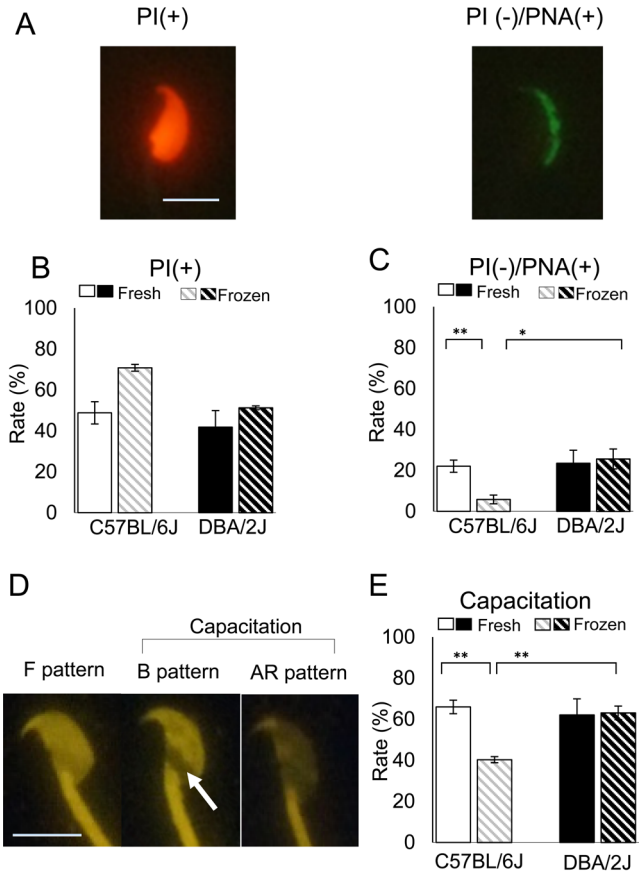

Fig. 4. Plasma membrane integrity, acrosomal status, and capacitation status of frozen-thawed spermatozoa from the parental strains. (A) Spermatozoa stained with PI and PNA conjugated with Alexa Fluor 488. The PI(+) pattern indicates spermatozoa with damaged plasma membranes. The PI(–)PNA(+) pattern indicates live spermatozoa ready to undergo an acrosome reaction (bar = 10 μm). (B) The rates of the PI(+) sperm in the parental strains (See PI(–) in Table 1). (C) The rates of the PI(–)PNA(+) sperm staining pattern in the parental strains (* $P < 0.05$; ** $P < 0.01$ by Tukey-Kramer test). See Table 1 for the result of two-way ANOVA. (D) Spermatozoa stained with CTC. The F pattern has uniform fluorescence over the sperm head (uncapacitated). The B pattern shows fluorescence on the anterior portion of the head and a dark band over the postacrosomal region (arrow) (capacitated but not acrosome-reacted). The AR pattern shows no or little fluorescence over the whole surface of the head (capacitated and acrosome-reacted). Spermatozoa with the B and AR patterns are considered to be capacitated. (E) The rates of capacitated spermatozoa in the parental strains (** $P < 0.01$ by Tukey-Kramer test). See Table 1 for the result of two-way ANOVA.

AR staining; Fig. 5). In particular, the AR pattern showed a correlation coefficient (r) of only 0.22, suggesting that acrosome-reacted spermatozoa after preincubation might not participate efficiently in fertilization. However, in IVF experiments using fresh spermatozoa, acrosome-reacted spermatozoa could pass through the cumulus layer and reached the zona very quickly [43]. It is probable that fresh spermatozoa and frozen-thawed spermatozoa might behave differently because freezing-thawing might change sperm physiology even with minimum damage. Our results suggest that the appearance of the B pattern after preincubation is a reliable index for optimization of the IVF protocol using frozen-thawed spermatozoa from different mouse strains. This was also the case with the PI(–)/PNA(+) staining pattern, which represented live spermatozoa ready to undergo the acrosome reaction. This rate also had a high correlation with the fertilization rate and might reflect a population of frozen-thawed spermatozoa with the highest chance to fertilize oocytes.

In our analysis, the parameters linked to sperm motility did not show any significant correlations with the relative fertilization rate. This might have been caused by the difference in the sperm populations used for these two kinds of analyses. For IVF, actively motile spermatozoa were collected from the periphery of the preincubation drop, whereas those for motility tests were collected from a stirred drop in which the sperm population was more homogenous. Indeed, when fresh spermatozoa were used for experiments, there were significant correlations between the fertilization rate and sperm motility parameters, probably because of the high viability of spermatozoa within the entire preincubation drop (data not shown).

With the advent of new techniques for IVF using frozen-thawed spermatozoa, such as the use of MBCD and GSH, sperm cryopreservation is now practically applicable for most mouse strains, including gene-modified mice from the B6J background. Sperm samples can be stored safely in LN_2 for many years and transported efficiently to other laboratories. However, it is important to study the mechanisms underlying cryodamage to spermatozoa because use of frozen-thawed spermatozoa for IVF or artificial insemination in other animals, such as pigs is sometimes impractical because of high individual

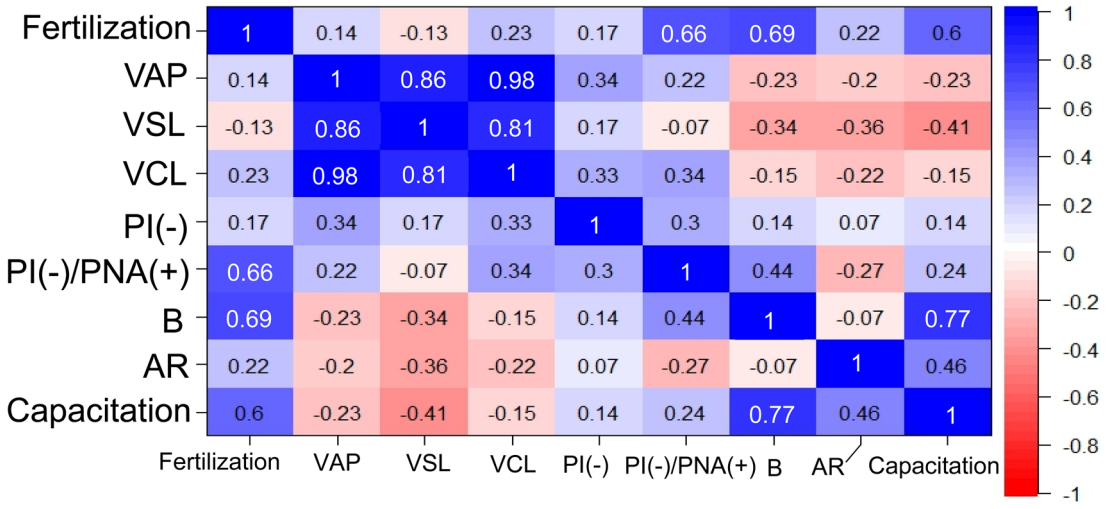

Fig. 5. Correlations between the fertilization rates and sperm-related parameters calculated using data from the RI, B6J, and D2J strains of mice. White numbers indicate the presence of significant differences ($P < 0.05$ for Pearson's correlation coefficient r).

Table 5. Mouse sperm staining for the plasmatic membrane, acrosome, and capacitation status in C57BL/6J, DBA/2J, and BXD RI mice

Strain	No. of males	Spermatozoa	PI(–) (%)	PI(–)/PNA(+) (%)	F pattern (%)	B pattern (%)	AR pattern (%)	Capacitation (%)
C57BL/6J	6	Fresh	57.5 ± 3.8	22.1 ± 3.0 ^{a}	34.0 ± 3.2 ^{a}	52.2 ± 3.3 ^{a}	13.7 ± 2.1	66.0 ± 3.2 ^{a}
	6	Frozen	29.8 ± 7.1	5.8 ± 2.1 ^{bA}	59.7 ± 1.7 ^{bc}	24.6 ± 1.5 ^{bA}	15.6 ± 1.5	40.3 ± 1.7 ^{bc}
DBA/2J	6	Fresh	61.7 ± 8.0	23.5 ± 6.4	37.9 ± 6.5	50.1 ± 7.8	12.0 ± 4.2	62.1 ± 6.5
	6	Frozen	48.8 ± 7.4	25.6 ± 4.9 ^{B}	36.9 ± 3.0 ^{d}	45.6 ± 3.3 ^{B}	17.4 ± 4.2	63.1 ± 3.0 ^{d}
BXD-8	6	Fresh	52.0 ± 9.7	15.6 ± 4.5	36.2 ± 6.4	53.5 ± 5.4	10.3 ± 2.9	63.8 ± 6.4
	6	Frozen	31.8 ± 3.2	6.9 ± 1.1	46.1 ± 2.9	33.5 ± 3.6	20.4 ± 2.5	53.9 ± 2.9
BXD-11	6	Fresh	41.5 ± 4.9	17.0 ± 2.4	34.6 ± 4.7	56.6 ± 3.5	8.7 ± 1.4	65.4 ± 4.7
	6	Frozen	31.2 ± 4.5	12.0 ± 3.8	48.8 ± 3.6	35.5 ± 2.9	15.7 ± 2.4	51.2 ± 3.6
BXD-12	5	Fresh	51.9 ± 6.3	18.1 ± 3.7	37.8 ± 5.0	53.2 ± 4.0	9.0 ± 2.0	62.2 ± 5.0
	5	Frozen	34.1 ± 5.9	12.8 ± 1.3	45.4 ± 6.1	37.5 ± 6.7	17.2 ± 3.9	54.6 ± 6.1
BXD-15	6	Fresh	62.7 ± 2.4	27.5 ± 1.6	33.4 ± 2.6	55.0 ± 4.2	11.6 ± 2.7	66.6 ± 2.6
	6	Frozen	30.3 ± 5.5	12.7 ± 2.8	29.8 ± 4.5	46.3 ± 5.8	23.8 ± 3.1	70.2 ± 4.5
BXD-19	6	Fresh	49.9 ± 5.6	13.6 ± 2.6	43.1 ± 5.6	45.7 ± 5.8	11.2 ± 1.2	56.9 ± 5.6
	6	Frozen	32.0 ± 3.0	11.9 ± 1.5	36.7 ± 2.5	45.7 ± 3.0	17.7 ± 3.6	63.3 ± 2.5
BXD-27	6	Fresh	54.5 ± 4.2	17.0 ± 2.4	51.4 ± 5.5	35.5 ± 4.3	13.1 ± 2.2	48.6 ± 5.5
	6	Frozen	36.0 ± 3.3	8.3 ± 2.2	48.8 ± 4.4	23.0 ± 5.3	28.2 ± 5.3	51.2 ± 4.4
BXD-31	6	Fresh	63.0 ± 5.9	13.3 ± 4.0	36.9 ± 2.7	50.6 ± 3.7	12.4 ± 1.2	63.1 ± 2.7
	6	Frozen	30.8 ± 4.6	11.5 ± 1.9	36.6 ± 4.7	44.0 ± 4.3	19.4 ± 1.7	63.4 ± 4.7
BXD-32	6	Fresh	43.8 ± 6.2	9.1 ± 2.7	27.8 ± 3.5	60.9 ± 4.1	11.3 ± 1.7	72.2 ± 3.5
	6	Frozen	26.1 ± 2.9	13.8 ± 2.6	35.5 ± 4.5	43.0 ± 4.8	21.5 ± 0.6	64.5 ± 4.5

Values are means ± SEMs. Different superscripts within the column indicate significant differences ($^{a,b;\ c,d}$ $P<0.01$; $^{A,\ B}$ $P<0.05$, For PI(–)/PNA(+), Kruskal-Wallis test was applied. For the F pattern and the B pattern, Tukey-Kramer test was applied. See Table 1). Multiple comparisons were not applied for PI(–) and the AR pattern because of the absence of a significant interaction between factors (see Table 1).

variability [44]. The genetic information obtained in this study will provide key information for improving sperm cryopreservation of species in which QTL analysis is difficult to perform.

Acknowledgments

The eight BXD RI strains and the D2J strain used in this study were provided by the RIKEN BioResource Center with the support of the National Bio-Resource Project of MEXT, Japan.

References

1. **Whittingham DG, Leibo SP, Mazur P.** Survival of mouse embryos frozen to -196 ° and -269 ° C. *Science* 1972; **178**: 411–414. [Medline] [CrossRef]
2. **Whittingham DG.** Embryo banks in the future of developmental genetics. *Genetics* 1974; **78**: 395–402. [Medline]
3. **Mochida K, Hasegawa A, Ogura A.** Recent technical breakthroughs for ARTs in mice. *J Mam Ova Res* 2017; **34**: 13–21. [CrossRef]
4. **Yokoyama M, Akiba H, Katsuki M, Nomura T.** Production of normal young following transfer of mouse embryos obtained by in vitro fertilization using cryopreserved spermatozoa. *Jikken Dobutsu* 1990; **39**: 125–128 (in Japanese). [Medline]
5. **Byers SL, Payson SJ, Taft RA.** Performance of ten inbred mouse strains following assisted reproductive technologies (ARTs). *Theriogenology* 2006; **65**: 1716–1726. [Medline] [CrossRef]
6. **Thornton CE, Brown SD, Glenister PH.** Large numbers of mice established by in vitro fertilization with cryopreserved spermatozoa: implications and applications for genetic resource banks, mutagenesis screens, and mouse backcrosses. *Mamm Genome* 1999; **10**: 987–992. [Medline] [CrossRef]
7. **Ostermeier GC, Wiles MV, Farley JS, Taft RA.** Conserving, distributing and managing genetically modified mouse lines by sperm cryopreservation. *PLoS ONE* 2008; **3**: e2792. [Medline] [CrossRef]
8. **Yoshiki A, Ike F, Mekada K, Kitaura Y, Nakata H, Hiraiwa N, Mochida K, Ijuin M, Kadota M, Murakami A, Ogura A, Abe K, Moriwaki K, Obata Y.** The mouse resources at the RIKEN BioResource center. *Exp Anim* 2009; **58**: 85–96. [Medline] [CrossRef]
9. **Tao J, Du J, Kleinhans FW, Critser ES, Mazur P, Critser JK.** The effect of collection temperature, cooling rate and warming rate on chilling injury and cryopreservation of mouse spermatozoa. *J Reprod Fertil* 1995; **104**: 231–236. [Medline] [CrossRef]
10. **Walters EM, Men H, Agca Y, Mullen SF, Critser ES, Critser JK.** Osmotic tolerance of mouse spermatozoa from various genetic backgrounds: acrosome integrity, membrane integrity, and maintenance of motility. *Cryobiology* 2005; **50**: 193–205. [Medline] [CrossRef]
11. **Tada N, Sato M, Yamanoi J, Mizorogi T, Kasai K, Ogawa S.** Cryopreservation of mouse spermatozoa in the presence of raffinose and glycerol. *J Reprod Fertil* 1990; **89**: 511–516. [Medline] [CrossRef]
12. **Sztein JM, Farley JS, Mobraaten LE.** In vitro fertilization with cryopreserved inbred mouse sperm. *Biol Reprod* 2000; **63**: 1774–1780. [Medline] [CrossRef]
13. **Hasegawa A, Mochida K, Tomishima T, Inoue K, Ogura A.** Microdroplet in vitro fertilization can reduce the number of spermatozoa necessary for fertilizing oocytes. *J Reprod Dev* 2014; **60**:187–193. [Medline] [CrossRef]
14. **Songsasen N, Leibo SP.** Cryopreservation of mouse spermatozoa. I. Effect of seeding on fertilizing ability of cryopreserved spermatozoa. *Cryobiology* 1997; **35**: 240–254. [Medline] [CrossRef]
15. **Nishizono H, Shioda M, Takeo T, Irie T, Nakagata N.** Decrease of fertilizing ability of mouse spermatozoa after freezing and thawing is related to cellular injury. *Biol Reprod* 2004; **71**: 973–978. [Medline] [CrossRef]
16. **Nakagata N, Takeshima T.** Cryopreservation of mouse spermatozoa from inbred and F1 hybrid strains. *Jikken Dobutsu* 1993; **42**: 317–320. [Medline]
17. **Choi YH, Toyoda Y.** Cyclodextrin removes cholesterol from mouse sperm and induces capacitation in a protein-free medium. *Biol Reprod* 1998; **59**: 1328–1333. [Medline] [CrossRef]
18. **Davis BK, Byrne R, Bedigian K.** Studies on the mechanism of capacitation: albumin-mediated changes in plasma membrane lipids during in vitro incubation of rat sperm cells. *Proc Natl Acad Sci USA* 1980; **77**: 1546–1550. [Medline] [CrossRef]
19. **Takeo T, Hoshii T, Kondo Y, Toyodome H, Arima H, Yamamura K, Irie T, Nakagata N.** Methyl-beta-cyclodextrin improves fertilizing ability of C57BL/6 mouse sperm after freezing and thawing by facilitating cholesterol efflux from the cells. *Biol Reprod* 2008; **78**: 546–551. [Medline] [CrossRef]
20. **Takeo T, Nakagata N.** Combination medium of cryoprotective agents containing L-glutamine and methyl-beta-cyclodextrin in a preincubation medium yields a high fertilization rate for cryopreserved C57BL/6J mouse sperm. *Lab Anim* 2010; **44**: 132–137. [Medline] [CrossRef]
21. **Takeo T, Nakagata N.** Reduced glutathione enhances fertility of frozen/thawed C57BL/6 mouse sperm after exposure to methyl-beta-cyclodextrin. *Biol Reprod* 2011; **85**: 1066–1072. [Medline] [CrossRef]
22. **Bath ML.** Inhibition of in vitro fertilizing capacity of cryopreserved mouse sperm by factors released by damaged sperm, and stimulation by glutathione. *PLoS One* 2010; **5**: e9387. [Medline] [CrossRef]
23. **Hasegawa A, Yonezawa K, Ohta A, Mochida K, Ogura A.** Optimization of a protocol for cryopreservation of mouse spermatozoa using cryotubes. *J Reprod Dev* 2012; **58**: 156–161. [Medline] [CrossRef]
24. **Taylor BA, Wnek C, Kotlus BS, Roemer N, MacTaggart T, Phillips SJ.** Genotyping new BXD recombinant inbred mouse strains and comparison of BXD and consensus maps. *Mamm Genome* 1999; **10**: 335–348. [Medline] [CrossRef]
25. **Peirce JL, Lu L, Gu J, Silver LM, Williams RW.** A new set of BXD recombinant inbred lines from advanced intercross populations in mice. *BMC Genet* 2004; **5**: 7. [Medline] [CrossRef]
26. **Hasegawa A, Mochida K, Inoue H, Noda Y, Endo T, Watanabe G, Ogura A.** High-yield superovulation in adult mice by anti-inhibin serum treatment combined with estrous cycle synchronization. *Biol Reprod* 2016; **94**: 21. [Medline] [CrossRef]
27. **Quinn P, Kerin JF, Warnes GM.** Improved pregnancy rate in human in vitro fertilization with the use of a medium based on the composition of human tubal fluid. *Fertil Steril* 1985; **44**: 493–498. [Medline] [CrossRef]
28. **Chatot CL, Ziomek CA, Bavister BD, Lewis JL, Torres I.** An improved culture medium supports development of random-bred 1-cell mouse embryos in vitro. *J Reprod Fertil* 1989; **86**: 679–688. [Medline] [CrossRef]
29. **Ogura A, Wakayama T, Suzuki O, Shin TY, Matsuda J, Kobayashi Y.** Chromosomes of mouse primary spermatocytes undergo meiotic divisions after incorporation into homologous immature oocytes. *Zygote* 1997; **5**: 177–182. [Medline] [CrossRef]
30. **Cheng F-P, Fazeli A, Voorhout WF, Marks A, Bevers MM, Colenbrander B.** Use of peanut agglutinin to assess the acrosomal status and the zona pellucida-induced acrosome reaction in stallion spermatozoa. *J Androl* 1996; **17**: 674–682. [Medline]
31. **Ward CR, Storey BT.** Determination of the time course of capacitation in mouse spermatozoa using a chlortetracycline fluorescence assay. *Dev Biol* 1984; **104**: 287–296. [Medline] [CrossRef]
32. **Fraser LR, McDermott CA.** Ca(2+)-related changes in the mouse sperm capacitation state: a possible role for Ca(2+)-ATPase. *J Reprod Fertil* 1992; **96**: 363–377. [Medline] [CrossRef]
33. **Fuller SJ, Whittingham DG.** Capacitation-like changes occur in mouse spermatozoa cooled to low temperatures. *Mol Reprod Dev* 1997; **46**: 318–324. [Medline] [CrossRef]
34. **Chesler EJ, Lu L, Wang J, Williams RW, Manly KF.** WebQTL: rapid exploratory analysis of gene expression and genetic networks for brain and behavior. *Nat Neurosci* 2004; **7**: 485–486. [Medline] [CrossRef]
35. **Alberts R, Schughart K.** QTLminer: identifying genes regulating quantitative traits. *BMC Bioinformatics* 2010; **11**: 516. [Medline] [CrossRef]
36. **Nedelko T, Kollmus H, Klawonn F, Spijker S, Lu L, Heßman M, Alberts R, Williams RW, Schughart K.** Distinct gene loci control the host response to influenza H1N1 virus infection in a time-dependent manner. *BMC Genomics* 2012; **13**: 411. [Medline] [CrossRef]
37. **Millman MS, Caswell AH, Haynes DH.** Kinetics of chlorotetracycline permeation in fragmented, ATPase-rich sarcoplasmic reticulum. *Membr Biochem* 1980; **3**: 291–315. [Medline] [CrossRef]
38. **Zídek V, Musilová A, Pintír J, Simáková M, Pravenec M.** Genetic dissection of testicular weight in the mouse with the BXD recombinant inbred strains. *Mamm Genome* 1998; **9**: 503–505. [Medline] [CrossRef]
39. **Cheng Q, Seltzer Z, Sima C, Lakschevitz FS, Glogauer M.** Quantitative trait loci and candidate genes for neutrophil recruitment in sterile inflammation mapped in AXB-BXA recombinant inbred mice. *PLoS ONE* 2015; **10**: e0124117. [Medline] [CrossRef]
40. **Courtemanche N, Gifford SM, Simpson MA, Pollard TD, Koleske AJ.** Abl2/Abl-related gene stabilizes actin filaments, stimulates actin branching by actin-related protein 2/3 complex, and promotes actin filament severing by cofilin. *J Biol Chem* 2015; **290**: 4038–4046. [Medline] [CrossRef]
41. **Lechtenberg BC, Mace PD, Riedl SJ.** Structural mechanisms in NLR inflammasome signaling. *Curr Opin Struct Biol* 2014; **29**: 17–25. [Medline] [CrossRef]
42. **Minutoli L, Antonuccio P, Irrera N, Rinaldi M, Bitto A, Marini H, Pizzino G, Romeo C, Pisani A, Santoro G, Puzzolo D, Magno C, Squadrito F, Micali A, Altavilla D.** NLRP3 Inflammasome Involvement in the organ damage and impaired spermatogenesis induced by testicular ischemia and reperfusion in mice. *J Pharmacol Exp Ther* 2015; **355**: 370–380. [Medline] [CrossRef]
43. **Hino T, Muro Y, Tamura-Nakano M, Okabe M, Tateno H, Yanagimachi R.** The Behavior and Acrosomal status of mouse spermatozoa in vitro, and within the oviduct during fertilization after natural mating. *Biol Reprod* 2016; **95**: 50. [Medline] [CrossRef]
44. **Yeste M.** Sperm cryopreservation update: Cryodamage, markers, and factors affecting the sperm freezability in pigs. *Theriogenology* 2016; **85**: 47–64. [Medline] [CrossRef]